Proceedings of the 9h World Congress on Civil, Structural, and Environmental Engineering (CSEE 2024)
London, United Kingdom – April 14-16, 2024
Paper No. ICSECT 147
DOI: 10.11159/icsect24.147

Compressive Behavior of Normal Strength Concrete Column Strengthened With Reinforced Ultra-High-Performance Concrete

Yasser E. Ibrahim[1], AIB Farouk[2], Jinsong Zhu[2], S.I. Haruna[1], Mohammed Al-samawi[2], Mustapha Abdulhadi[3]
[1]Engineering Management Department, College of Engineering,
Prince Sultan University, Riyadh 11586, Saudi Arabia
ymansour@psu.edu.sa (Y.E.I), aifg1986@tju.edu.cn, (AIB Farouk),
[2]School of Civil Engineering,
Tianjin University, Tianjin 300350, China
jszhu@tju.edu.cn (J. Zhu),
[3]Department of Civil Engineering,
Chulalongkorn University, Bangkok, Thailand.

Abstract - Ultra-high-performance concrete (UHPC) and normal strength concrete (NSC) are concrete materials with high compatibility characteristics. This paper presents the experimental and numerical study on the uniaxial compression behavior of NSC columns strengthened using UHPC. The main idea of the proposed strengthening technique is to optimize the UHPC and enhance the ultimate capacity, impermeability, and crack resistance of the damaged column. Fourteen (14) NSC columns strengthened with UHPC were tested. The influence of longitudinal groove geometry and volumetric ratio of shear reinforcement on the failure mode, ultimate capacity, displacement, initial stiffness, ductility index, and ultimate strain of the composite column was investigated. Increasing the groove size will increase the axial resistance and improve the ductility of the strengthened NSC column. Decreasing the shear reinforcement ratio does not affect the axial strength of the column. The developed FEM can accurately simulate the behavior of the column strengthened with UHPC using the proposed technique.

***Keywords*:** Compressive behavior, UHPC strengthening, grooved contact surface, finite element analysis

1. Introduction

The low tensile and compressive strength and high permeability characteristics make normal-strength concrete (NSC) structures deteriorate quickly, especially in alkaline environments. As a result, the concrete deteriorates, and reinforcement corrode [1]. The spalling of the concrete cover results in the exposure of longitudinal reinforcing bars. Therefore, the mechanical and durability performance will be seriously affected. The permanent deformation of a structured column affects its serviceability and endangers the restoration process, resulting in total replacement.

Using ultra-high-performance concrete (UHPC) in construction has proven a successful method of overcoming conventional NSC [2]. UHPC poses higher durability characteristics, such as high impermeability of aggressive substances such as chloride and sulfate [3]. Furthermore, UHPC is characterized by high strength, enhanced crack resistance, and extended service life [4]. Therefore, the mechanical properties and durability characteristics of UHPC par exceed the normal strength concrete (NSC) [5]. Most existing bridges exceed their design life span and require efficient repair or replacement methodologies, not to mention the new ones to meet existing populations [6]. Therefore, there is a demand for strengthening techniques that enhance the resistance and robustness of damaged NSC columns subjected to extreme events.

The strengthening effect of UHPC on damaged NSC columns has been investigated by many researchers [7]. A single approach of increasing the outer thickness of the UHPC to improve the strength, ductility, axial stiffness, energy, confinement effect of UHPC, and absorption of damaged concrete was adopted. However, because of the difference in mechanical properties between the damaged NSC column and the repaired UHPC layer, increasing the outer thickness of the UHPC will cause a shift of the critical section to an undesired location when inappropriate UHPC thickness is used. In addition, the thickness of the UHPC layer determines the overall cost of the strengthening process. A new technique that optimizes the thickness of UHPC to reduce the maintenance cost while improving the structural integrity of the damaged NSC is necessary.

This study proposed a new strengthening technique. Instead of increasing the outer layer of the UHPC to improve the performance of the damaged NSC, this technique first introduced an internal longitudinal grooving on the damaged NSC. Then, the UHPC layer with a constant thickness *t* overlays a damaged NSC column. The influence of grove thickness and shear reinforcement volumetric ratio on the compressive behavior of the strengthened concrete column was investigated. A finite element model was established to simulate the behavior of the strengthened concrete. Figure 1 presents the proposed strengthening technique.

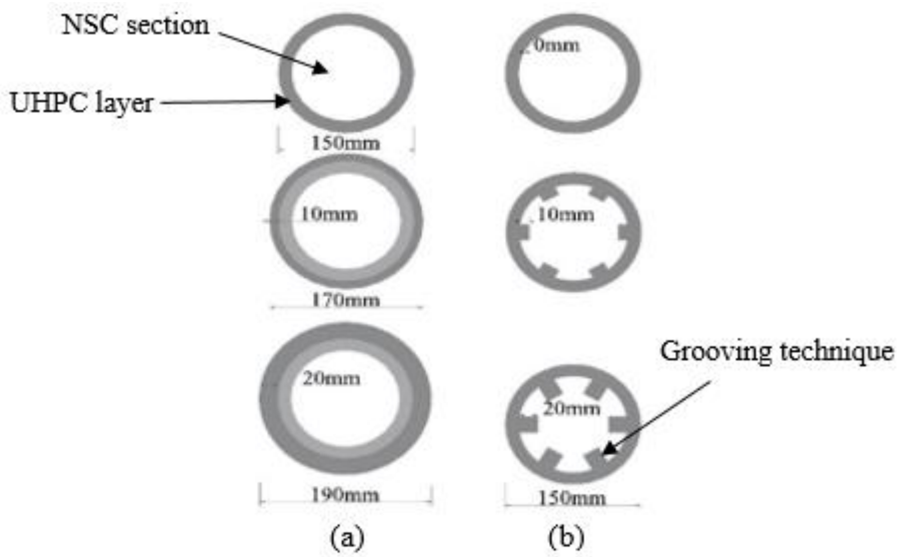

Fig. 1: Strengthening technique (a) conventional approach (b) proposed method.

2. Testing Program

2.1 Specimens detail

Table 1 presents the details of the NSC column strengthened with UHPC. The overall geometry of the column is 400 mm in height and 160 mm in diameter. 10 mm diameter of grade 60 (Gr 60) reinforcement was used. The G and V refer to the longitudinal groove size and rebar spacing.

Table 1. Details of the columns strengthened with UHPC

Specimens	Groove Geometry	*s*(mm)	Number of duplicates
G0	0	75	2
G10	10	75	3
G20	20	75	3
V150	20	150	3
V225	20	225	3

2.2 Material properties and Sample preparations

Tables 2 and 3 present the mixed proportion and mechanical properties of the UHPC and NSC. The design compressive strength of NSC and UHPC is 30 and 120 MPa, respectively. The NSC comprises ordinary Portland cement, water, and fine and coarse aggregate. The UHPC comprises premixed power of 1.18 mm aggregate size, quartz, silica fume, superplasticizer, and 2% straight steel fibers.

Table 2 The NSC and UHPC mixed proportion

Material	Cement	Quartz	Crushed Stone	Superplasticizer	Silica fume	Water	W/C ratio
UHPC	898	1258	-	17	225	202	0.18
NSC	360	665	1157	-	-	190	0.53

Table 3. NSC and UHPC Mechanical properties

Material	fc' (MPa)	E (GPa)	ft (MPa)	ρ (Kg/m^3)	L (mm)	ϕ (mm)
NSC	36.77	29.17	4.30	2400	-	-
UHPC	125.23	41.28	7.22	2500	-	-
Steel Fiber	-	200	2500	7850	13	0.2

The column specimen was fabricated in sequence. Fig. 2 presents the sequence of specimen preparation and strengthening process. The NSC formwork with internal grooving was first prepared using a 110 mm PVC pipe. Then, the plain NSC was cast and removed, followed by a rebar arrangement. The UHPC was then cast and cured at room temperature. The 120 Ω resistance was installed vertically and horizontally to measure the axial and lateral strain.

Fig. 2: Specimen preparations

2.3 Test Setup and Instrumentation

Fig. 3 presents the test setup of the strengthened column. Four LVDTs were used to measure the axial and lateral stains of the column under compression. MTS 300T machine was used for the test. The machine recorded the axial load, while the LVDT and strain were used to measure the columns' deformation and strain. The displacement loading type was used until failure.

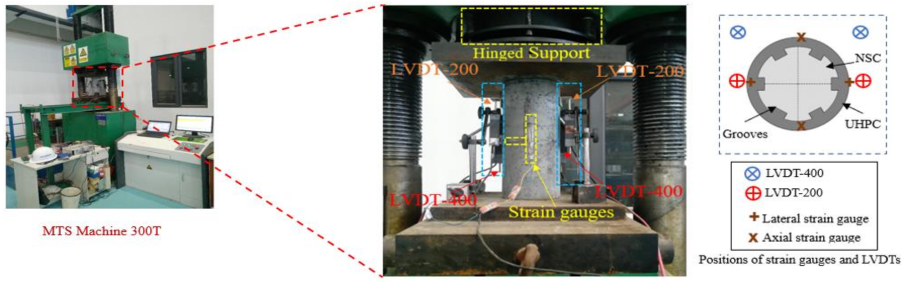

Fig. 4 Instrumentation and test setup

3. Results and Discussion

3.1 Load Strain Behavior

Table 4 presents the load-strain relationship of the NSC column strengthened with UHPC using the proposed technique. The table summarize the peak load P(kN), ultimate load Pu (kN), axial strain at peak load εy (με), the axial strain at ultimate load εyu (με), and lateral strain at ultimate load εx (με). There is an increase in the axial load and axial and lateral strain with increasing groove size, while increasing the shear reinforcement spacing increases the lateral strain and decreases the axial strain of the column.

Table 4 Axial load-strain relationship

Specimens	P(kN)	Pu(kN)	εy (με)	εyu (με)	εx (με)
G0-1	910.32	768.63	3000	3900	2500
G0-2	911.46	774.35	3200	4100	1900
G10-1	1312.23	1117.15	2200	2700	1500
G10-2	1218.59	1036.39	2300	4000	2300
G10-3	1354.74	1151.53	2500	3200	2300
G20-1	1194.33	1071.06	2100	3300	3700
G20-2	1071.28	926.20	5600	3600	2000
G20-3	1195.23	1021.02	2200	3600	2900
V150-1	1171.62	879.26	2600	2700	200
V150-2	1085.45	922 .64	1900	2100	4000
V150-3	1179.36	1002.45	2600	2700	3500
V225-1	1089.52	937.67	1900	2100	6100
V225-2	1277.05	1085.49	3200	3300	6500
V225-3	1275.55	1084.21	2900	3000	6300

3.2 Ductility index

The ductility index (δi) parameter was used to examine the ductility of the repaired concrete column. The ratio of the 85% column deformation to the ultimate deformation represents the ductility index of that column [8]. Therefore, it is expressed.

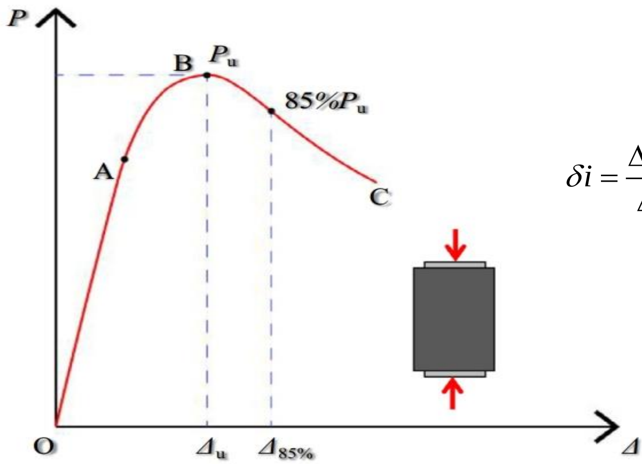

$$\delta i = \frac{\Delta_{0.85}}{\Delta_U} \tag{1}$$

Fig. 4. Ductility index properties

The influence of groove size and shear rebar ratio on the ductility index of the repaired column is presented in Figure 5. Increasing the groove size from 0 to 10 and 20 mm improves the ductility index by 8% and 17%, respectively. However, decreasing the shear reinforcement ratio from 0.17 to 0.15 and 0.13% has reduced the ductility index by 49.6% and 50.2%.

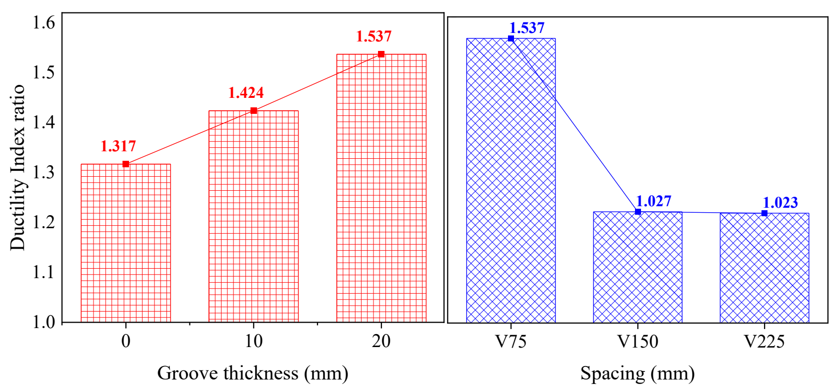

Fig. 5: Effect of (a) groove size and (b) shear rebar ratio on the ductility index

4. Finite Element Analysis

4.1 General

The finite element (FE) model helps to simulate the general behavior of the strengthened column using the developed approach. The ABAQUS software package [9] was used to simulate the behavior of the NSC column strengthened with UHPC using the developed approach. The concrete damage plasticity (CDP) was used to simulate the material behavior of UHPC and NSC. The constitutive model used by Farouk et al. [10] defined the uniaxial compression and tension of the concretes and steel bars. The CDPM parameters for NSC and UHPC used in this study are similar to those used by the authors in [11]. Figure 6, 7, and 8 represents the stress-strain behavior of the NSC, UHPC, and steel bars, respectively.

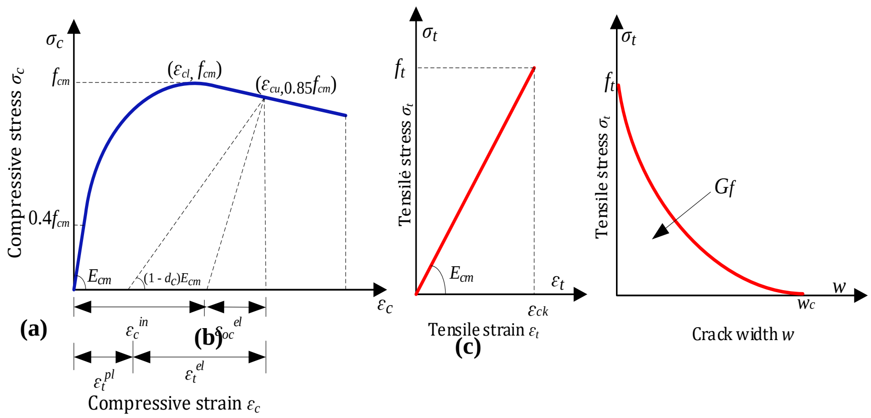

Fig. 6: Concrete-damaged plasticity model of NSC in (a) stress-strain in compression, (b) stress-strain in tension, and (c) stress-crack width.

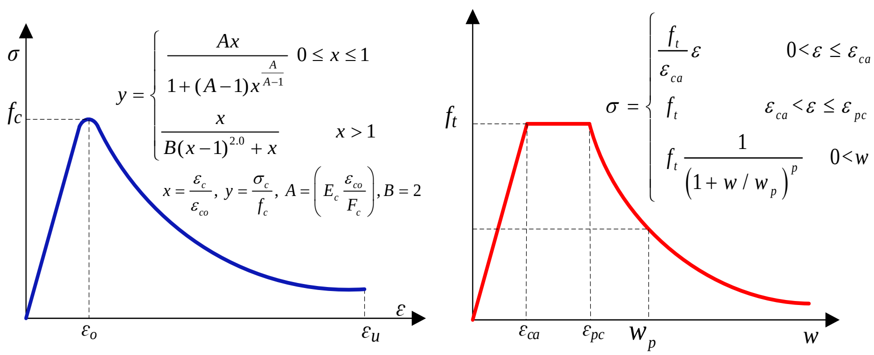

$$y=\begin{cases}\dfrac{Ax}{1+(A-1)x^{\frac{A}{A-1}}} & 0\le x\le 1\\[2ex] \dfrac{x}{B(x-1)^{2.0}+x} & x>1\end{cases}$$

$$x=\frac{\varepsilon_c}{\varepsilon_{co}},\ y=\frac{\sigma_c}{f_c},\ A=\left(E_c\frac{\varepsilon_{co}}{F_c}\right),B=2$$

$$\sigma=\begin{cases}\dfrac{f_t}{\varepsilon_{ca}}\varepsilon & 0<\varepsilon\le\varepsilon_{ca}\\ f_t & \varepsilon_{ca}<\varepsilon\le\varepsilon_{pc}\\ f_t\dfrac{1}{\left(1+w/w_p\right)^p} & 0<w\end{cases}$$

Fig. 7: CDP model of UHPC in (a) compression and (b) in tension

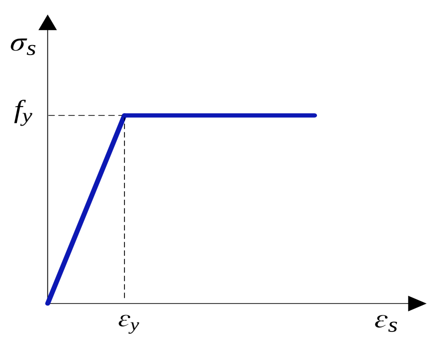

Fig. 8: Constitutive relationship of steel rebars

For more accurate prediction, applying the proper boundary conditions, element type, mesh size, and material behavior is critical. Therefore, the NSC and UHPC are designed as three-dimensional eight-nodes with reduced integration points (C3D8R), while the reinforcement bars are designed as truss elements (T3D2). The convergence criteria were used in selecting the mesh size, and a 10 mm size was selected. Surface-to-surface interaction was used to define the contact between UHPC and NSC. The concrete is the host region, while the rebars are the embedment region. The displacement-controlled loading was applied as the loading type.

4.2 Model Validation

The failure pattern between the experimental test and numerical modeling was compared, similar failure mode between the experiment and FEM was observed in all the specimens. The concrete crushing and UHPC tensile failures were observed in all the specimens. The cracks were observed at the mid-height of the specimens; however, the intensity of the cracks was reduced by increasing the internal groove size. Figure 10 presents the load-deformation curve between the experimental and FEM. The figure indicates the agreement between the experiment and FEM.

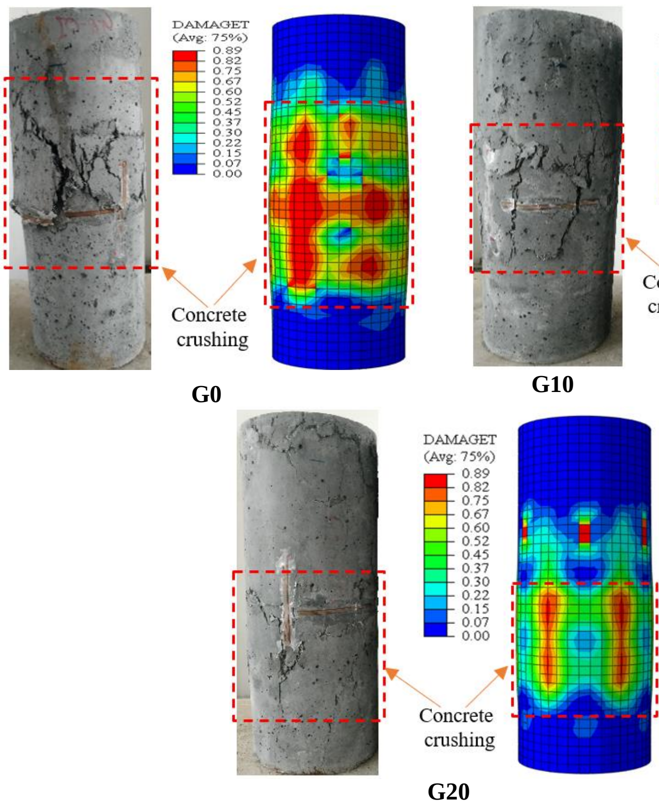

Fig. 9: Failure Mode between experiment and FEM

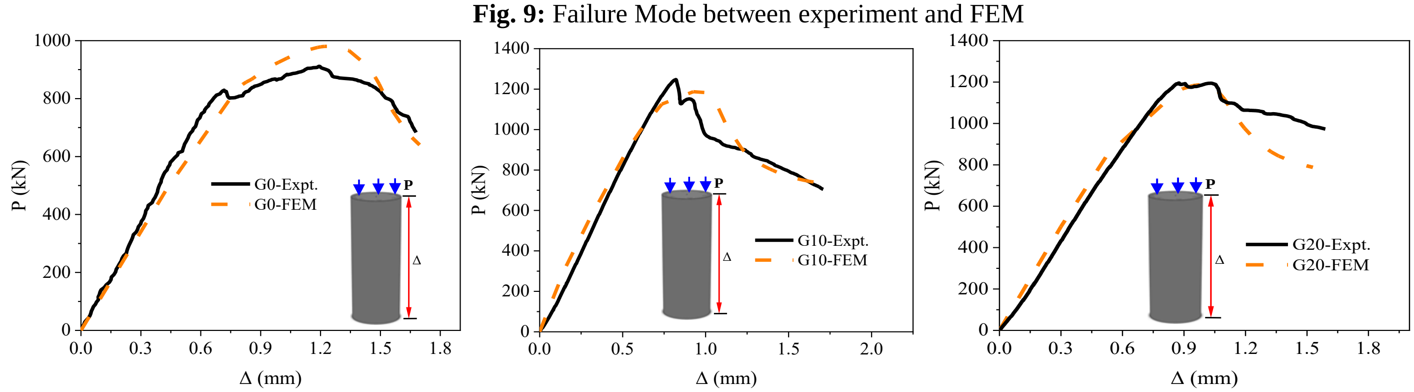

Fig. 10: P-Δ curve between Experimental and FEM

5. Conclusion

This paper proposed a new strengthening technique for damaged NSC with UHPC. The idea of the proposed method is to optimize the UHPC and increase the integrity of NSC. Fourteen (14) NSC stub columns were strengthened with UHPC using different internal groove sizes and shear reinforcement spacing. An axial compression test was conducted to test the performance of the strengthened column. The finite element model was developed and validated using experimental tests. The following conclusions were drawn based on the experimental and FEM results.

1. The proposed strengthening technique can improve the axial performance of the NSC. The experimental results show that the column capacity is increased by increasing the internal groove size. The 20 mm groove size can improve the axial capacity and ductility index of the strengthened column by 27% and 17 %, respectively.
2. The developed FEM simulates the behavior of the column with acceptable accuracy and can be used for parametric analysis. The idea of the proposed method is to optimize the UHPC and increase the integrity of NSC.
3. The effect of groove size and rebar spacing other than those used in the experiment can be investigated. Other parameters, such as different loading conditions and combined shear and bending effects, can be checked

Acknowledgment

This work was supported by the National Natural Science Foundation of China [grant number 52078333] and the Tianjin Transportation Science and Technology Development Plan Project [grant number 2019B-21]. The conference fees and attendance are supported by Prince Sultan University. These supports are gratefully acknowledged. Any opinions, findings, conclusions, or recommendations expressed in this paper are those of the authors and do not necessarily reflect those of the sponsor.

References

[1] X. Shi, N. Xie, K. Fortune, and J. Gong, “Durability of steel reinforced concrete in chloride environments: An overview,” *Constr. Build. Mater.*, vol. 30, pp. 125–138, 2012.

[2] N. Naeimi and M. A. Moustafa, “Numerical modeling and design sensitivity of structural and seismic behavior of UHPC bridge piers,” *Eng. Struct.*, vol. 219, p. 110792, 2020.

[3] C. Magureanu, I. Sosa, C. Negrutiu, and B. Heghes, “Mechanical properties and durability of ultra-high-performance concrete,” *ACI Mater. J.*, vol. 109, no. 2, pp. 177–184, 2012.

[4] M. Farzad, M. Shafieifar, and A. Azizinamini, “Experimental and numerical study on bond strength between conventional concrete and Ultra High-Performance Concrete (UHPC),” *Eng. Struct.*, vol. 186, pp. 297–305, 2019.

[5] F. Baby, B. Graybeal, P. Marchand, and F. Toutlemonde, “Proposed flexural test method and associated inverse analysis for ultra-high-performance fiber-reinforced concrete,” *ACI Mater. J.*, vol. 109, no. 5, p. 545, 2012.

[6] A. Sriram and S. Sri, “Quantifying Bonding Characteristics between UHPC and Normal-Strength Concrete for Bridge Deck Application,” *J. Bridg. Eng.*, vol. 24, no. 6, p. 4019041, Jun. 2019.

[7] H. Tian, Z. Zhou, Y. Zhang, and Y. Wei, “Axial behavior of reinforced concrete column with ultra-high performance concrete stay-in-place formwork,” *Eng. Struct.*, vol. 210, p. 110403, 2020.

[8] J.-B. Yan, X.-T. Wang, and T. Wang, “Compressive behaviour of normal weight concrete confined by the steel face plates in SCS sandwich wall,” *Constr. Build. Mater.*, vol. 171, pp. 437–454, 2018.

[9] A. Dassault, “6.14-Abaqus Analysis User’s Manual,” *Dassault Systèmes Simulia Corp*, 2014.

[10] A. I. B. Farouk, J. Zhu, and G. Yuhui, “Finite element analysis of the shear performance of box-groove interface of ultra-high-performance concrete (UHPC)-normal strength concrete (NSC) composite girder,” *Innov. Infrastruct. Solut.*, vol. 7, no. 3, p. 212, 2022.

[11] A. I. B. Farouk, W. Rong, and J. Zhu, “Compressive behavior of ultra-high-performance-normal strength concrete (UHPC-NSC) column with the longitudinal grooved contact surface,” *J. Build. Eng.*, vol. 68, p. 106074, Jun. 2023.